HHS Public Access

Author manuscript

Clin Cancer Res. Author manuscript; available in PMC 2017 May 01.

Published in final edited form as:

Clin Cancer Res. 2016 May 1; 22(9): 2250–2260. doi:10.1158/1078-0432.CCR-15-2276.

Strategically timing inhibition of phosphatidylinositol 3-kinase to maximize therapeutic index in estrogen receptor alpha-positive, *PIK3CA*-mutant breast cancer

Wei Yang[1], **Sarah R. Hosford**[1], **Lloye M. Dillon**[1], **Kevin Shee**[1], **Stephanie C. Liu**[1], **Jennifer R. Bean**[1], **Laurent Salphati**[2], **Jodie Pang**[2], **Xiaolin Zhang**[2], **Michelle A. Nannini**[3], **Eugene Demidenko**[4], **Darcy Bates**[5], **Lionel D. Lewis**[5], **Jonathan D. Marotti**[6,7], **Alan R. Eastman**[1], and **Todd W. Miller**[1,7,8]

[1]Dept. of Pharmacology & Toxicology, Norris Cotton Cancer Center, Geisel School of Medicine at Dartmouth, Lebanon, NH

[2]Depts. of Drug Metabolism & Pharmacokinetics, Genentech, Inc., South San Francisco, California

[3]Dept. of Translational Oncology, Genentech, Inc., South San Francisco, California

[4]Dept. of Community & Family Medicine, Norris Cotton Cancer Center, Geisel School of Medicine at Dartmouth, Lebanon, NH

[5]Dept. of Medicine, Norris Cotton Cancer Center, Geisel School of Medicine at Dartmouth, Lebanon, NH

[6]Dept. of Pathology, Norris Cotton Cancer Center, Geisel School of Medicine at Dartmouth, Lebanon, NH

[7]Dept. of Comprehensive Breast Program, Norris Cotton Cancer Center, Geisel School of Medicine at Dartmouth, Lebanon, NH

Abstract

Purpose—Phosphatidylinositol 3-kinase (PI3K) inhibitors are being developed for the treatment of estrogen receptor α (ER)-positive breast cancer in combination with anti-estrogens. Understanding the temporal response and pharmacodynamic effects of PI3K inhibition in ER+ breast cancer will provide rationale for treatment scheduling to maximize therapeutic index.

Experimental Design—Anti-estrogen-sensitive and -resistant ER+ human breast cancer cell lines, and mice bearing *PIK3CA*-mutant xenografts were treated with the anti-estrogen fulvestrant, the PI3K inhibitor GDC-0941 (pictilisib; varied doses/schedules that provided similar amounts of drug each week), or combinations. Cell viability, signaling pathway inhibition, proliferation, apoptosis, tumor volume, and GDC-0941 concentrations in plasma and tumors were temporally measured.

[8]To whom correspondence should be addressed. **Corresponding author**. Todd W. Miller, Dartmouth-Hitchcock Medical Center One Medical Center Dr. HB-7936, Lebanon, NH 03756, Phone: (603) 653-9284, Todd.W.Miller@Dartmouth.edu.

Conflicts of interest: LS, JP, XZ, and MNP are employees of Genentech, Inc.

Results—Treatment with the combination of fulvestrant and GDC-0941, regardless of dose/schedule, was significantly more effective than single-agent treatments in fulvestrant-resistant tumors. Short-term, complete PI3K inhibition blocked cell growth *in vitro* more effectively than chronic, incomplete inhibition. Longer-term PI3K inhibition hypersensitized cells to growth factor signaling upon drug withdrawal. Different schedules of GDC-0941 elicited similar tumor responses. While weekly high-dose GDC-0941 with fulvestrant continuously suppressed PI3K signaling for 72 hours, inducing a bolus of apoptosis and inhibiting proliferation, PI3K reactivation upon GDC-0941 washout induced a proliferative burst. Fulvestrant with daily low-dose GDC-0941 metronomically suppressed PI3K for 6–9 hours/day, repeatedly inducing small amounts of apoptosis and temporarily inhibiting proliferation, followed by proliferative rebound compared to fulvestrant alone.

Conclusions—Continuous and metronomic PI3K inhibition elicit robust anti-cancer effects in ER+, *PIK3CA*-mutant breast cancer. Clinical exploration of alternate treatment schedules of PI3K inhibitors with anti-estrogens is warranted.

Keywords

PI3K; ER; anti-estrogen; breast cancer

Introduction

Approximately 70% of breast cancers express estrogen receptor α (ER) and/or progesterone receptor (PR), which typically indicate a degree of estrogen dependence. Patients with hormone receptor-positive breast cancer are treated with anti-estrogen therapies [*e.g.*, tamoxifen, fulvestrant (fulv), aromatase inhibitors (AIs)] that inhibit ER signaling. While adjuvant therapy with anti-estrogens prevents cancer recurrence, 1/3 of patients develop anti-estrogen-resistant advanced breast cancer that is rarely cured by approved therapies (1, 2).

We and others have shown that hyperactivation of the phosphatidylinositol 3-kinase (PI3K)/AKT/mechanistic target of rapamycin (mTOR) pathway in preclinical models and human breast tumors promotes anti-estrogen resistance (3, 4). PI3K is the most frequently aberrantly activated pathway in cancer, and alterations in genes encoding PI3K pathway proteins occur in >70% of ER+ breast cancers [data extracted from refs. (5, 6)]. PI3K pathway activation promotes cell growth, proliferation, survival, and migration. Small molecule-mediated inhibition of PI3K, AKT, and/or mTOR suppresses anti-estrogen-resistant growth of ER+ breast cancer cells and xenografts, particularly in models harboring gain-of-function mutations in *PIK3CA* [encodes the PI3K subunit p110α, the most commonly altered gene in ER+ breast cancer (5)] or loss-of-function mutations in *PTEN* (encodes a phosphatase that antagonizes PI3K signaling) (3, 7–9). The approved mTOR complex 1 (mTORC1) inhibitor everolimus delays disease progression in ER+ breast cancer in combination with the AI exemestane (10). However, mTORC1 inhibition blocks negative feedback on activators of PI3K, promoting PI3K activation and cell survival (11–13). Thus, direct inhibitors of PI3K may be more effective.

PI3K inhibitors are being developed clinically for the treatment of breast and other cancers (14–18). Recommended Phase II doses (RP2Ds) of the Class IA pan-PI3K inhibitors

BKM120 (buparlisib) and GDC-0941 (pictilisib) were established through Phase I dose-escalation studies that determined maximum tolerated doses using daily treatment schedules. At RP2Ds, Grade 3/4 adverse events occurred in 24–46% of patients treated with BKM-120 or GDC-0941, either alone or in combination with an anti-estrogen, leading to treatment discontinuation or dose reductions in a similar proportion of cases (14–18). In humans, these drugs have long plasma half-lives (~40 and ~16 h, respectively), so daily dosing provides continuous drug exposure at concentrations that are inconsistently sufficient to robustly inhibit PI3K/AKT/mTOR (16, 17). While it is generally thought that continuous target inhibition is required for anti-cancer effects of kinase inhibitors (19), mechanistic rationale is often lacking. Indeed, transient interruption of oncogenic signaling pathways has been shown to elicit robust anti-cancer effects in models of chronic myeloid leukemia (CML; imatinib and dasatinib inhibit BCR-ABL) and HER2-positive breast cancer (lapatinib inhibits EGFR and HER2) (20, 21). Intermittent dosing with lapatinib elicits a similar response rate as continuous dosing in patients with solid tumors (22). Intermittent treatment with the BRAF inhibitor vemurafenib and the MEK inhibitor cobimetinib induced prolonged clinical responses in a patient with $BRAF^{V600K}$-mutant melanoma and *NRAS*-mutant leukemia (23). While imatinib is typically administered on a daily schedule, weekly dosing prevented recurrence in 7/7 patients with chronic eosinophilic leukemia (24). Intermittent high-dose treatment has also been shown to increase central nervous system penetration of small molecules such as the EGFR inhibitor erlotinib to treat lung cancer metastases (25). In order to provide mechanistic rationale for clinical testing of doses/schedules of PI3K inhibitors that may increase therapeutic index, we determined the temporal effects of PI3K inhibition in models of ER+/HER2−/*PIK3CA*-mutant breast cancer.

Material and Methods

Cell lines

All parental cell lines were obtained from ATCC, cultured in DMEM/10% FBS (Hyclone), and passaged for <3 months before analysis. Fulv-resistant (FR) MCF-7 (MCF-7/FR) and T47D (T47D/FR) cells were a gift from Matthew Ellis (Washington Univ.) and maintained in DMEM/10% FBS (Hyclone) with 1 μM fulv (Tocris Bioscience); cell lines were authenticated by mutational profiling using a 541-gene panel. ZR75-1/FR cells were generated by culturing ZR75-1 cells with 1 μM fulv for 4 months. T47D/PTREX-Bim cells were a gift from Anthony Faber (Virginia Commonwealth Univ.).

Sulforhodamine B (SRB) assay

Cells were seeded at 3,000–5,000/well in 96-well plates. The next day, cells were treated with 0–2 μM GDC-0941 (kindly provided by Genentech) +/− 1 μM fulv for up to 5 d. Relative numbers of adherent cells were determined by SRB staining as previously described (26).

Xenograft studies

Animal studies were approved by the Dartmouth College IACUC. Female NOD-scid/IL2R$\gamma^{-/-}$ (NSG; NOD.Cg-Prkdcscid Il2rgtm1Wjl/SzJ) mice (6–7 wks old; obtained from the Norris Cotton Cancer Center Transgenic & Genetic Construct Shared Resource) were

subcutaneously injected with 5–10×10^6 MCF-7 cells in matrigel (BD Biosciences), or orthotopically implanted with ~8-mm^3 fragments of serially transplanted HCI-003 patient-derived xenograft tissue [a gift from Alana Welm, Univ. of Utah (27)] in the inguinal #4 mammary fat pad; mice were subcutaneously implanted on the same day with a 17β-estradiol pellet (0.72 mg, 60-day-release; Innovative Research of America). In mice subcutaneously injected with T47D/FR cells, subcutaneous administration of 5 mg/wk fulv was initiated on the same day [clinical formulation; provides ER inhibition in MCF-7 tumors for ≥8 d (data not shown); kindly provided by AstraZeneca]. Mice bearing tumors 500–1,000 mm^3 were randomized to treatment with vehicle, 5 mg/kg fulv QW, GDC-0941 (100 mg/kg QDx5d QW, 100 mg/kg BIDx3d QW, or 800 mg/kg QW, p.o. in 100 μL 0.5% methylcellulose/0.2%Tween-80), and combinations. Tumor volumes were measured twice weekly using calipers (volume = $length^2$×width/2). Tumors were harvested and cut in pieces for snap-freezing or formalin fixation followed by paraffin embedding (FFPE).

Immunoblotting

Immunoblotting of protein extracts from cells and frozen tumor fragments was performed as previously described (28). Relative levels of (phospho)proteins were measured by densitometry using ImageJ software.

Immunohistochemistry (IHC)

Five-micron sections of FFPE tumor tissue were used for H&E staining, IHC with antibodies against Ki67 (Biocare Medical) or geminin (Santa Cruz Biotechnology), and TUNEL (DeadEnd Colorimetric System; Promega). Proportions of positively stained cells were counted in 3 random microscopic fields (400× magnification) in each specimen.

Pharmacokinetic and pharmacodynamic analyses

Mice were treated with 100 or 800 mg/kg GDC-0941. Blood was collected by cardiac puncture at 0–72 h into tubes containing EDTA (0.5 M final concentration) as an anti-coagulant, and centrifuged at 2,000 × *g* for 5 min at 4°C. Plasma was removed and stored at −80°C.

A separate group of mice bearing MCF-7 tumors was treated with fulv. Three days later, mice were treated with GDC-0941 (100 mg/kg, 800 mg/kg, or 100 mg/kg at 0 and 12 h). Tumors were harvested at 0–72 h and snap-frozen. GDC-0941 concentrations in plasma and tumors were determined as previously described (29). Pharmacokinetic and pharmacodynamic parameters were estimated by analyzing GDC-0941 concentration or effect versus time using WinNonlin software. Pharmacokinetic and pharmacodynamic data were analyzed using a non-compartmental model and the log-linear trapezoidal rule. For pharmacokinetic parameters, Tmax and Cmax were the observed time to maximum concentration, and maximum concentration, respectively. The following pharmacokinetic parameters were calculated: area under the curve from zero to infinity [$AUC_{(0\text{-}inf)}$]; terminal elimination half-life ($T_{1/2}$); mean residence time (MRT). For apoptosis and proliferation, maximum impact (Amax for apoptosis; Pmax for proliferation) and time to reach maximum impact (Tmax) were the observed values, and area under the curve from 0–144 h [$AUC_{(0–144)}$] was calculated.

Statistical analyses

In vitro cell growth, tumor IHC and TUNEL data were analyzed by ANOVA followed by Bonferroni multiple comparison-adjusted post-hoc test between groups. To estimate progression/regression of tumors, the following linear mixed model was employed: $\log_{10}$(tumor volume) = a + b*t [refs. (30–32)]. The computation was carried out in statistical package R (33), using function 'lme' from library 'nlme.' The intercept of the linear model (a) for each treatment group in each tumor type estimates the $\log_{10}$(tumor volume) at time 0 (baseline), and the slope (b) estimates the rate of growth/reduction.

Additional methods are provided in Supplementary Information.

Results

Transient, complete inhibition of PI3K more effectively suppresses cell growth than continuous, partial PI3K inhibition

PI3K inhibitors exhibit little clinical efficacy as single agents (16–18), induce ER activation (Fig. S1), and are being tested in combination with anti-estrogens for the treatment of patients with ER+ breast cancer (14, 15). We first found that longer-term exposure to GDC-0941 induced PI3K hyperactivation (indicated by phospho-AKT levels) upon drug washout in MCF-7, ZR75-1, and T47D ER+/HER2− breast cancer cells (Fig. 1A). Similarly, longer-term exposure to GDC-0941 induced hypersensitivity to growth factor stimulation upon drug washout (Fig. 1B), suggesting that A) longer-term PI3K inhibition induces increases in PI3K activators, and B) that shorter-term PI3K inhibition might avoid such rebound effects upon drug washout. To determine the duration of PI3K inhibition required to induce anti-cancer effects in ER+ breast cancer, cells were treated with 0–2 μM GDC-0941 alone or in combination with 1 μM fulv for 0–120 h, followed by GDC-0941 washout. Relative numbers of viable cells were measured after 120 h. In *PIK3CA*-mutant ($p110\alpha^{E545K}$) MCF-7 cells, a 3- to 6-h exposure to pharmacologically achievable concentrations of GDC-0941 [1–2 μM (17)] decreased cell viability ≥50% (Fig. 1C). Continuous exposure to 1–2 μM GDC-0941 induced near-complete growth inhibition. In contrast, lower concentrations of GDC-0941 (≤0.25 μM) required longer durations of exposure (≥24 h) to appreciably decrease viability, reflecting a relationship between duration and magnitude of PI3K inhibition, and cell viability. Single-agent fulv effectively inhibited growth of MCF-7 cells (Fig. S2). Thus, we used fulv-resistant MCF-7/FR cells to assess the effects of fulv and GDC-0941 in combination. Although it has been reported that MCF-7 cells resistant to fulv exhibit hyperactivation of insulin-like growth factor-1 receptor (IGF-1R), HER2, and epidermal growth factor receptor (EGFR), indicating general upregulation of growth-stimulatory pathways (4), MCF-7/FR dose/exposure responses to GDC-0941 were similar to those seen in parental MCF-7 cells (Fig. 1D). Analyses in *PIK3CA*-mutant ($p110\alpha^{E545K}$) MDA-MB-361 cells, and PTEN-deficient ZR75-1 and ZR75-1/FR cells confirmed that more complete PI3K inhibition (1–2 μM GDC-0941) with shorter exposure (24–48 h) generally provides better growth inhibition than incomplete PI3K inhibition (0.25–0.5 μM) with chronic exposure (≥72 h) (Figs. 1C–D, S2). We did not observe these relationships in *PIK3CA*-mutant ($p110\alpha^{H1047R}$) T47D cells (Fig. S2), possibly due to a genetic deficiency in *BCL2L11* that encodes the pro-apoptotic protein Bim [Fig. S2

and ref. (34)]. Expression of exogenous Bim increased sensitivity to short-term treatment with 1–2 μM GDC-0941 (Fig. S2).

To monitor the kinetics of early apoptotic events, we used MCF-7 and ZR75-1 cells stably expressing a caspase-3/7-activatable luciferase reporter (35). Cells were treated +/− 1 μM fulv for 2 d before exposure to 1 μM GDC-0941 for 12, 24, or 36 h. While combination drug treatment increased caspase-3/7 reporter activity compared to either agent alone, short- and longer-term exposures to fulv/GDC-0941 provided similar degrees of reporter activity in MCF-7 (12, 24, and 36 h) and ZR75-1 cells (12 and 24 h) (Fig. S3). These data suggest that A) transient, complete inhibition of PI3K more effectively suppresses cell growth than continuous, partial inhibition, B) short- and longer-term complete PI3K inhibition elicit similar degrees of growth inhibition and apoptosis, and C) longer-term PI3K inhibition primes cells for PI3K hyperactivation upon drug washout.

Pharmacokinetics of GDC-0941

We next tested the hypothesis that infrequent, pulsatile, high-dose (*i.e.*, weekly) PI3K inhibition elicits greater anti-tumor effects than frequent, metronomic, low-dose (*i.e.*, daily) PI3K inhibition *in vivo*. GDC-0941 pharmacokinetic analyses were performed with a fulv treatment backbone. To allow time for downstream effects of fulv-mediated inhibition of ER transcriptional activity (Fig. S4), mice were treated with fulv at 3 d prior to administration of GDC-0941. GDC-0941 plasma concentrations peaked after 15–30 min (Fig. 2A and Table S1). With 100 mg/kg GDC-0941, plasma concentrations decreased to a plateau phase after 1 h, were maintained for 8 h (6.8–10.7 μM), and decreased below the limit of detection within 24 h. With 800 mg/kg GDC-0941, the plateau phase was maintained through 24 h (7.9–15 μM), and drug concentrations decreased below detectable limits within 72 h.

Since GDC-0941 plasma concentrations dropped sharply at 9 h after low-dose treatment (Fig. 2A), a third dosing schedule was included (100 mg/kg at 0 and 12 h) to provide near-continuous exposure with bi-daily dosing. Mice bearing MCF-7 xenografts were treated as above to assess tumor pharmacokinetics. Intratumor concentrations of GDC-0941 peaked at 9 h with low-dose and high-dose treatments, and at 21 h with two low-dose treatments. With low-dose GDC-0941, drug was undetectable at 18 h after a single dose, and after 36 h with a second dose (Fig. 2B and Table S1). With high-dose GDC-0941, intratumor drug concentrations declined between 9–48 h, decreasing below the detectable limit by 72 h. Pharmacokinetic parameter estimation revealed that high-dose GDC-0941 provided increased half-life ($T_{1/2}$), exposure [$AUC_{(0\text{-inf})}$], and mean residence time (MRT) compared to low dose GDC-0941 (Fig. 2B).

Pharmacodynamic effects of PI3K inhibition on ER+ breast tumors

Mice bearing MCF-7 xenografts were treated as in Fig. 2. It has been reported that baseline PI3K activity (as measured by P-AKT levels) and PI3K inhibitor-induced mTORC1 inhibition (as measured by decreased levels of P-S6) correlate with clinical response (36). Thus, we measured levels of P-AKT and P-S6 as markers of PI3K and mTORC1 activities, respectively. P-AKT and P-S6 levels were maximally suppressed after ~1 h of both low- and high-dose GDC-0941 treatments, and returned to baseline within 9 and 72 h, respectively

(Fig. 3A) while total AKT levels were unchanged (data not shown). P-AKT and P-S6 levels were inversely correlated with intratumor concentrations of GDC-0941 (Fig. S5). In agreement with *in vitro* findings (Fig. S1), the combination of fulv and GDC-0941 increased tumor cell apoptosis. PARP cleavage (marker of apoptosis) occurred within 1 and 3 h of high-dose and low-dose GDC-0941 treatments, respectively, and cleavage increased over time (Fig. 3A).

A second low-dose GDC-0941 treatment after 12 h provided continued inhibition of PI3K and mTORC1 for ≥21 h, and more PARP cleavage than a single low-dose treatment (Fig. 3B), suggesting that bi-daily low-dose treatment is sufficient to nearly continuously inhibit PI3K. As observed *in vitro* (Fig. 1A/B), markers of PI3K and mTORC1 activities rebounded above baseline after GDC-0941 washout (Fig. 3C and Fig. S6). For example, while PI3K inhibition decreased P-S6 levels at early time points, P-S6 increased above baseline within 1 d after daily or bi-daily low-dose treatments, and 3 d after a single high-dose treatment (Fig. S6). In sum, low- and high-dose GDC-0941 inhibit PI3K/mTORC1 signaling for 6–9 and 72 h, respectively, so bi-daily low-dose treatment should provide near-continuous pathway inhibition. However, drug washout permits pathway hyperactivation.

Longer-term PI3K inhibition increases apoptosis and suppresses proliferation in combination with anti-estrogen therapy in MCF-7 tumors

Tumors harvested from mice at 24, 36, and 48 h following one day of treatment with GDC-0941 (+/− fulv pretreatment) were analyzed by TUNEL to monitor apoptosis. Single agents induced minimal apoptosis (Fig. 4A and Fig. S7). In combination with fulv, one or two (0 and 12 h) low doses of GDC-0941 induced peak apoptosis in 6.7% and 15.9% of tumor cells at 24 h, respectively; apoptotic cell numbers declined thereafter. In contrast, high-dose GDC-0941 induced peak apoptosis at 48 h (30.1%); it is unclear whether this marked apoptosis is partially attributable to a lack of clearance of dead cells. Interestingly, apoptotic timing was associated with the presence of drug (compare Fig. 2B and Fig. 4A).

Ki67 has been widely used as a marker of proliferation, but non-mitotically active cells can express Ki67 in G1 phase. Thus, we also evaluated geminin positivity as a marker of cells in S/G2 phases, and geminin/Ki67 ratio indicates the proportion of proliferating cells in S/G2 (37). One or two low doses (0 and 12 h) of single-agent GDC-0941 significantly decreased tumor cell proliferation as measured by geminin/Ki67 ratio at 24 h (52.1% decreased to 29.1% and 31.6%, respectively), which rebounded by 48 h (37.7% and 36.4%) (Fig. 4B). High-dose GDC-0941 similarly blocked proliferation as a single agent, with continued inhibition through 48 h (52.1% to 19.3%). Single-agent fulv suppressed proliferation (34.9%), and combination treatment with GDC-0941/fulv further decreased geminin/Ki67 ratio at 24 h. Evaluation of geminin and Ki67 as individual markers showed similar patterns of drug effects (Fig. S8 and Fig. S9).

When GDC-0941 was cleared from tumors of mice co-treated with fulv, tumor cell proliferation rebounded above levels observed in tumors from fulv-treated mice (compare Fig. 2B and Fig. 4B); while we considered that this indicates synchronized S-phase entry of G1-arrested cells, further analyses (described below) indicated that these are likely genuine increases in proliferation. In contrast, fulv plus high-dose GDC-0941 suppressed

proliferation through 48 h. Taken together, these data suggest that A) temporal changes in tumor cell apoptosis and proliferation can be predicted based on GDC-0941 pharmacokinetics, B) fulv administered with daily low-dose GDC-0941 should continually promote G1 arrest and a modest degree of apoptosis, C) fulv plus bi-daily low-dose GDC-0941 should further increase apoptosis, and D) fulv plus weekly high-dose GDC-0941 should drastically suppress proliferation and induce apoptosis. However, evaluation of the longer-term effects of these treatments, particularly following GDC-0941 washout, requires a longer time course (below).

Intermittent, longer-term PI3K inhibition is as effective as metronomic PI3K inhibition in combination with anti-estrogen therapy against ER+/*PIK3CA*-mutant breast tumors

While we previously found that smaller MCF-7 tumors regress in response to fulv (38), larger tumors (500–1,000 mm^3) are generally unresponsive (Fig. S10 and Table S2). GDC-0941 was administered at doses/schedules that provided similar total amounts of drug (Fig. 5A). Different doses/schedules of single-agent GDC-0941 only slowed tumor growth without notable loss of body weight. Surprisingly, the combination of fulv and GDC-0941, regardless of dose/schedule, induced near-complete tumor regression in most cases (Fig. 5B, Fig. S10, and Table S2).

To validate observations in MCF-7 tumors, mice bearing *PIK3CA*-mutant ($p110\alpha^{H1047R}$, confirmed by DNA sequencing) T47D/FR xenografts treated with fulv from the time of cell implantation were randomized to different GDC-0941 doses/schedules. All GDC-0941 co-treatments induced tumor regression or stasis through 4.5 wk until daily low-dose GDC-0941-treated mice resumed tumor growth (Fig. 5C, Fig. S11, Fig. S12A, and Table S2). Withdrawal of fulv at 6.5 wk was associated with outgrowth of most tumors despite continued GDC-0941 treatment (Fig. S11), suggesting that combined targeting of PI3K and ER is required for disease control.

We then tested these treatments in mice bearing estrogen-dependent, ER+/HER2−/*PIK3CA*-mutant ($p110\alpha^{H1047R}$) HCI-003 patient-derived breast cancer xenografts. While fulv did not affect tumor growth, combined treatment with fulv and GDC-0941 (daily low-dose or weekly high-dose) induced tumor stasis (Fig. 5D, Fig. S12, Fig. S13, and Table S2). Notably, tumors from combination-treated mice showed large areas of central necrosis (Fig. S12), suggesting that anti-tumor effects were more significant than physically measureable.

Intermittent, longer-term inhibition of PI3K induces a wave of apoptosis and proliferative inhibition, with proliferative rebound after recovery of PI3K activity despite continued ER inhibition

Different doses/schedules of PI3K inhibition similarly induced tumor responses in combination with fulv (Fig. 5). However, pharmacodynamic data indicated that high-dose GDC-0941 more effectively increased apoptosis and suppressed proliferation compared to low-dose GDC-0941 (Fig. 4). Thus, we temporally profiled MCF-7 tumors from mice treated for up to 7 d. A single treatment of fulv plus high-dose GDC-0941 induced peak apoptosis at 48 h (30.1%), which dropped to baseline (2.7%) by 72 h when GDC-0941 was cleared, and below baseline thereafter (compare Fig. 2B and Fig. 6A). Fulv plus bi-daily

low-dose GDC-0941 (3 d on, 4 d off) induced peak apoptosis at 24 h (18.3%), and maintained apoptosis at ~10% until 72 h when GDC-0941 was cleared (compare Fig. 2B and Fig. 6A). Fulv plus daily low-dose GDC-0941 induced 8–10% apoptosis that was maintained for 72 h; despite continued metronomic PI3K inhibition (Fig. S6), apoptosis levels returned to baseline thereafter (Fig. 6A). These findings suggest that the bulk of apoptosis occurs within the first 3 d following initiation of PI3K inhibitor therapy. Pharmacodynamic modeling of apoptosis rate over the course of 7 d [$AUC_{(0–144)}$] revealed that a single high dose of GDC-0941 with fulv cumulatively induces more apoptosis that daily or bi-daily low-dose GDC-0941 regimens with fulv (Fig. 6A).

A single treatment with fulv plus high-dose GDC-0941 decreased tumor cell proliferation by 48 h (34.9% decreased to 11.46%), which rebounded above baseline following GDC-0941 washout (Fig. 6B, Fig. 2B, and Fig. S14). While it is conceivable that this washout-induced increase in geminin/Ki67 ratio reflects synchronized S-phase entry of G1-arrested cells, increased geminin/Ki67 ratio persisted for up to 7 d, suggesting that PI3K reactivation promotes proliferation. Fulv plus low-dose GDC-0941 (daily or bi-daily) modestly decreased proliferation, but geminin/Ki67 ratio increased above baseline after 2–3 d of treatment (Fig. 6B, Fig. 2B, and Fig. S14). $AUC_{(0–144)}$ generated from pharmacodynamic modeling showed that fulv plus daily low-dose GDC-0941 cumulatively inhibited tumor cell proliferation modestly better than bi-daily low-dose GDC-0941/fulv or a single high dose of GDC-0941/fulv within a one-week period (Fig. 6B). These results collectively indicate that different schedules of PI3K inhibition with anti-estrogen therapy provide similar anti-tumor efficacy due to cumulative effects on apoptosis and proliferation: 1) intermittent, longer-term PI3K inhibition (weekly high-dose GDC-0941) induces a burst of apoptosis and proliferative inhibition that rebounds above baseline upon PI3K reactivation; 2) metronomic PI3K inhibition (daily low-dose GDC-0941) induces smaller amounts of apoptosis and proliferative inhibition with less proliferative rebound.

Discussion

Herein, we demonstrate that both metronomic (daily) and intermittent (weekly) inhibition of PI3K in combination with an anti-estrogen induce regression of anti-estrogen-resistant, ER+/*PIK3CA*-mutant breast tumors. Combined targeting of ER and PI3K was significantly more effective than single-agent treatments. Detailed pharmacodynamic and pharmacokinetic profiling revealed that the majority of tumor cell apoptosis occurred early during the course of treatment, temporally correlating with PI3K inhibition. *In vitro* analyses showed that both short- and long-term inhibition of PI3K effectively reduced cell viability. These findings support the clinical exploration of different treatment schedules of PI3K inhibitors that may increase therapeutic index.

Kinase inhibitors are often developed with pharmacokinetic properties and/or clinical dosing schedules that provide continuous drug exposure and target inhibition. The theory underlying this “occupancy-driven pharmacology” is that longer occupation of an enzyme active site by drug will translate into increased clinical efficacy. While drug target inhibition is often confirmed in blood, skin, or tumor biopsies in early-phase clinical studies, temporal analysis of molecular effects in tumors is rarely feasible. Thus, mechanistic rationale for

dosing schedules is often lacking. Given that PI3K inhibitor treatment regimens being tested clinically induce significant toxicity and inconsistently provide robust pathway inhibition (14–18, 36), we sought to determine whether anti-tumor efficacy could be achieved using alternate, pharmacodynamically-informed treatment schedules. Indeed, weekly treatment with a high dose of GDC-0941 (800 mg/kg), daily treatment with a lower dose (100 mg/kg), or bi-daily treatment with a lower dose for 3 consecutive days per week (100 mg/kg BIDx3d QW) all induced similar tumor responses when combined with fulv in 3 models of ER+ breast cancer (Fig. 5, Fig. S10, Fig. S11, Fig. S13, and Table S2). Weekly high-dose and bi-daily low-dose treatments provided continuous PI3K inhibition for 48–60 h (Fig. 3 and Fig. S6), while daily low-dose treatment metronomically inhibited PI3K for 6–9 h/d. In correlation, intermittent (weekly and bi-daily) PI3K inhibition induced a bolus of apoptosis followed by a rebound in tumor cell proliferation, while metronomic (daily) PI3K inhibition repeatedly induced small amounts of apoptosis (Figs. 4A, 6A). Genes encoding PI3K activators (*e.g.*, IGF-1R, HER3) are transcriptionally upregulated in response to long-term (≥4 h), but not short-term (≤2 h), PI3K inhibition via activation of FoxO transcription factors (39). Long-term PI3K inhibition also upregulates ER levels and activity (Fig. S1A), and ER promotes *IGF1R* transcription. Thus, the hyperproliferative tumor response to PI3K reactivation in mice treated with high-dose GDC-0941 (Fig. 6B and Fig. S14) may be related to the hypersensitization of PI3K to growth factor stimulation following prolonged PI3K inhibition (Fig. 1A/B). We conclude that the sum of anti-proliferative and pro-apoptotic effects of these treatment regimens are similar, providing comparable tumor responses. Whether the PI3K reactivation-associated hyperproliferative tumor response promotes an aggressive tumor phenotype that may affect disease progression requires further detailed study.

We found that MCF-7 tumors regressed to near completion with combined inhibition of ER and PI3K, while T47D/FR and HCI-003 tumors either slightly regressed or growth-arrested (Fig. 5, Fig. S10, Fig. S11, and Fig. S13). While inhibitors of oncogenic effector kinases (*e.g.*, PI3K, MEK) frequently inhibit cancer cell proliferation, apoptosis is required for regression of solid tumors (34). Hata *et al.* recently reported that the ratio of pro-apoptotic (*e.g.*, Bim) to anti-apoptotic (*e.g.*, Bcl-2, Bcl-xL) proteins dictates cell fate in response to PI3K and MEK inhibitors (40). We found that A) MCF-7 tumors express a higher ratio of Bim:Bcl-2/Bcl-xL than T47D/FR or HCI-003 tumors, potentially “priming” MCF-7 tumors for apoptosis (41), B) T47D/FR tumors are Bim-deficient, and C) HCI-003 tumors express high levels of Bcl-xL (Fig. S15 and Fig. S1). Therefore, T47D/FR and HCI-003 tumors are predicted to regress if co-treated with a drug that sufficiently increases the balance of pro-apoptotic/anti-apoptotic proteins (*e.g.*, the Bcl-2/Bcl-xL inhibitor navitoclax). These data also suggest that the nature of clinical response (regression versus stable disease) to ER/PI3K inhibition may be predictable based on the ratio of pro-apoptotic/anti-apoptotic proteins.

In ER+ breast cancer models, phosphorylation of ribosomal protein S6 is often controlled by a PI3K signaling cascade, placing mTORC1 and cap-dependent translation under PI3K control. Elkabets *et al.* reported that treatment-induced decreases in P-S6 levels are predictive of response to PI3K/p110α inhibition in *PIK3CA*-mutant breast cancer cells and human tumors, and mTORC1 reactivation is associated with drug resistance (36). While

fulv/GDC-0941 initially decreased P-S6 levels in tumor models tested herein, P-S6 rebounded independently of P-AKT in some cases (Fig. 3 and Fig. S6). These findings suggest that A) mTORC1 activation quickly becomes disconnected from PI3K/AKT due to signaling reprogramming and/or clonal selection, and B) using P-S6 as a pharmacodynamic biomarker to predict clinical response may be complicated by timing of assessment and compensatory mTORC1-activating pathways. Furthermore, therapeutic targeting of both mTORC1 and PI3K (*i.e.*, "vertical inhibition," using drugs that target the same pathway) may provide additional benefit beyond PI3K inhibition in combination with an anti-estrogen in ER+ breast cancer.

In summary, our analysis of ER+/*PIK3CA*-mutant breast tumors suggests that anti-estrogen therapy with different schedules of pharmacologic PI3K inhibition, while all efficacious, elicit different pharmacodynamic effects in tumors. While continuous exposure to a PI3K inhibitor may provide chronic pathway suppression in patients, this strategy may increase systemic toxicity; shorter-term, intermittent PI3K inhibition may provide less systemic toxicity with similar clinical response. This concept may be extrapolated to the development of other signaling pathway modulators. These findings provide rationale for clinical exploration of alternate treatment schedules with kinase inhibitors that may increase therapeutic index in patients.

Supplementary Material

Refer to Web version on PubMed Central for supplementary material.

Acknowledgments

We thank the following Norris Cotton Cancer Center Shared Resources for assistance: Transgenic & Genetic Construct, Clinical Pharmacology, Pathology Translational Research, and Immunoassays & Flow Cytometry.

Financial support

Financial support was provided by the American Cancer Society (RSG-13-292-01-TBE to TWM), and NIH (R00CA142899 to TWM; Dartmouth College Norris Cotton Cancer Center Support Grant P30CA023108).

References

1. Ferlay JS, Bray F, Forman D, Mathers C, Parkin DM. Estimates of worldwide burden of cancer in 2008: GLOBOCAN 2008. Internat J Cancer. 2010:2893–2917.
2. Davies C, Godwin J, Gray R, Clarke M, Cutter D, et al. Early Breast Cancer Trialists' Collaborative G. Relevance of breast cancer hormone receptors and other factors to the efficacy of adjuvant tamoxifen: patient-level meta-analysis of randomised trials. Lancet. 2011; 378:771–784. [PubMed: 21802721]
3. Miller TW, Hennessy BT, Gonzalez-Angulo AM, Fox EM, Mills GB, Chen H, et al. Hyperactivation of phosphatidylinositol-3 kinase promotes escape from hormone dependence in estrogen receptor-positive human breast cancer. J Clin Invest. 2010; 120:2406–2413. [PubMed: 20530877]
4. Miller TW, Balko JM, Arteaga CL. Phosphatidylinositol 3-kinase and antiestrogen resistance in breast cancer. J Clin Oncol. 2011; 29:4452–4461. [PubMed: 22010023]
5. TCGA. Comprehensive molecular portraits of human breast tumours. Nature. 2012; 490:61–70. [PubMed: 23000897]

6. Cerami E, Gao J, Dogrusoz U, Gross BE, Sumer SO, Aksoy BA, et al. The cBio cancer genomics portal: an open platform for exploring multidimensional cancer genomics data. Cancer Discov. 2012; 2:401–404. [PubMed: 22588877]
7. Miller TW, Balko JM, Fox EM, Ghazoui Z, Dunbier A, Anderson H, et al. ERalpha-dependent E2F transcription can mediate resistance to estrogen deprivation in human breast cancer. Cancer Discov. 2011; 1:338–351. [PubMed: 22049316]
8. Miller TW, Perez-Torres M, Narasanna A, Guix M, Stal O, Perez-Tenorio G, et al. Loss of Phosphatase and Tensin homologue deleted on chromosome 10 engages ErbB3 and insulin-like growth factor-I receptor signaling to promote antiestrogen resistance in breast cancer. Cancer Res. 2009; 69:4192–4201. [PubMed: 19435893]
9. O'Brien C, Wallin JJ, Sampath D, GuhaThakurta D, Savage H, Punnoose EA, et al. Predictive biomarkers of sensitivity to the phosphatidylinositol 3' kinase inhibitor GDC-0941 in breast cancer preclinical models. Clin Cancer Res. 2010; 16:3670–3683. [PubMed: 20453058]
10. Baselga J, Campone M, Piccart M, Burris HA 3rd, Rugo HS, Sahmoud T, et al. Everolimus in postmenopausal hormone-receptor-positive advanced breast cancer. N Engl J Med. 2012; 366:520–529. [PubMed: 22149876]
11. Miller TW, Forbes JT, Shah C, Wyatt SK, Manning HC, Olivares MG, et al. Inhibition of mammalian target of rapamycin is required for optimal antitumor effect of HER2 inhibitors against HER2-overexpressing cancer cells. Clin Cancer Res. 2009; 15:7266–7276. [PubMed: 19934303]
12. O'Reilly KE, Rojo F, She QB, Solit D, Mills GB, Smith D, et al. mTOR inhibition induces upstream receptor tyrosine kinase signaling and activates Akt. Cancer Res. 2006; 66:1500–1508. [PubMed: 16452206]
13. Carracedo A, Ma L, Teruya-Feldstein J, Rojo F, Salmena L, Alimonti A, et al. Inhibition of mTORC1 leads to MAPK pathway activation through a PI3K-dependent feedback loop in human cancer. J Clin Invest. 2008; 118:3065–3074. [PubMed: 18725988]
14. Mayer IA, Abramson VG, Isakoff SJ, Forero A, Balko JM, Kuba MG, et al. Stand up to cancer phase Ib study of pan-phosphoinositide-3-kinase inhibitor buparlisib with letrozole in estrogen receptor-positive/human epidermal growth factor receptor 2-negative metastatic breast cancer. J Clin Oncol. 2014; 32:1202–1209. [PubMed: 24663045]
15. Krop, I.; Johnston, S.; Mayer, IA.; Dickler, M.; Ganju, V.; Forero-Torres, A.; Melichar, B.; Morales, S.; de Boer, R.; Gendreau, S.; Derynck, M.; Lackner, M.; Spoerke, J.; Yeh, R-F.; Levy, G.; Ng, V.; O'Brien, C.; Savage, H.; Xiao, Y.; Wilson, T.; Lee, SC.; Petrakova, K.; Vallentin, S.; Yardley, D.; Ellis, M.; Piccart, M.; Perez, EA.; Winer, E.; Schmid, P. The FERGI phase II study of the PI3K inhibitor pictilisib (GDC-0941) plus fulvestrant vs fulvestrant plus placebo in patients with ER+, aromatase inhibitor (AI)-resistant advanced or metastatic breast cancer – Part I results; Presented at the San Antonio Breast Cancer Symposium; 2014. Abstract S2-02.
16. Bendell JC, Rodon J, Burris HA, de Jonge M, Verweij J, Birle D, et al. Phase I, dose-escalation study of BKM120, an oral pan-Class I PI3K inhibitor, in patients with advanced solid tumors. J Clin Oncol. 2012; 30:282–290. [PubMed: 22162589]
17. Sarker D, Ang JE, Baird R, Kristeleit R, Shah K, Moreno V, et al. First-in-human phase I study of pictilisib (GDC-0941), a potent pan-class I phosphatidylinositol-3-kinase (PI3K) inhibitor, in patients with advanced solid tumors. Clin Cancer Res. 2015; 21:77–86. [PubMed: 25370471]
18. Rodon J, Brana I, Siu LL, De Jonge MJ, Homji N, Mills D, et al. Phase I dose-escalation and -expansion study of buparlisib (BKM120), an oral pan-Class I PI3K inhibitor, in patients with advanced solid tumors. Invest New Drugs. 2014; 32:670–681. [PubMed: 24652201]
19. Bradshaw JM, McFarland JM, Paavilainen VO, Bisconte A, Tam D, Phan VT, et al. Prolonged and tunable residence time using reversible covalent kinase inhibitors. Nature chemical biology. 2015; 11:525–531. [PubMed: 26006010]
20. Amin DN, Sergina N, Ahuja D, McMahon M, Blair JA, Wang D, et al. Resiliency and vulnerability in the HER2–HER3 tumorigenic driver. Sci Transl Med. 2010; 2:16ra7.
21. Shah NP, Kasap C, Weier C, Balbas M, Nicoll JM, Bleickardt E, et al. Transient potent BCR-ABL inhibition is sufficient to commit chronic myeloid leukemia cells irreversibly to apoptosis. Cancer Cell. 2008; 14:485–493. [PubMed: 19061839]

22. Chew HK, Somlo G, Mack PC, Gitlitz B, Gandour-Edwards R, Christensen S, et al. Phase I study of continuous and intermittent schedules of lapatinib in combination with vinorelbine in solid tumors. Ann Oncol. 2012; 23:1023–1029. [PubMed: 21778300]
23. Abdel-Wahab O, Klimek VM, Gaskell AA, Viale A, Cheng D, Kim E, et al. Efficacy of intermittent combined RAF and MEK inhibition in a patient with concurrent BRAF- and NRAS-mutant malignancies. Cancer Discov. 2014; 4:538–545. [PubMed: 24589925]
24. Helbig G, Stella-Holowiecka B, Majewski M, Calbecka M, Gajkowska J, Klimkiewicz R, et al. A single weekly dose of imatinib is sufficient to induce and maintain remission of chronic eosinophilic leukaemia in FIP1L1-PDGFRA-expressing patients. Br J Haematol. 2008; 141:200–204. [PubMed: 18307562]
25. Grommes C, Oxnard GR, Kris MG, Miller VA, Pao W, Holodny AI, et al. "Pulsatile" high-dose weekly erlotinib for CNS metastases from EGFR mutant non-small cell lung cancer. Neuro-oncology. 2011; 13:1364–1369. [PubMed: 21865399]
26. Vichai V, Kirtikara K. Sulforhodamine B colorimetric assay for cytotoxicity screening. Nat Protoc. 2006; 1:1112–1116. [PubMed: 17406391]
27. DeRose YS, Wang G, Lin YC, Bernard PS, Buys SS, Ebbert MT, et al. Tumor grafts derived from women with breast cancer authentically reflect tumor pathology, growth, metastasis and disease outcomes. Nat. Med. 2011; 17:1514–1520. [PubMed: 22019887]
28. Dillon LM, Bean JR, Yang W, Shee K, Symonds LK, Balko JM, et al. P-REX1 creates a positive feedback loop to activate growth factor receptor, PI3K/AKT and MEK/ERK signaling in breast cancer. Oncogene. 2014
29. Salphati L, Wong H, Belvin M, Bradford D, Edgar KA, Prior WW, et al. Pharmacokinetic-pharmacodynamic modeling of tumor growth inhibition and biomarker modulation by the novel phosphatidylinositol 3-kinase inhibitor GDC-0941. Drug Metab Dispos. 2010; 38:1436–1442. [PubMed: 20538720]
30. Demidenko E. The assessment of tumour response to treatment. Applied Statistics. 2006; 55:365–377.
31. Demidenko E. Three endpoints of in vivo tumour radiobiology and their statistical estimation. Internat J Radiat Biol. 2010; 86:164–173.
32. Demidenko, E. Mixed Models: Theory and Applications with R. 2nd. New York: Wiley; 2013.
33. Team, RC. R: A language and environment for statistical computing. Vienna, Austria: R Foundation for Statistical Computing; 2014.
34. Faber AC, Corcoran RB, Ebi H, Sequist LV, Waltman BA, Chung E, et al. BIM expression in treatment-naive cancers predicts responsiveness to kinase inhibitors. Cancer Discov. 2011; 1:352–365. [PubMed: 22145099]
35. Coppola JM, Ross BD, Rehemtulla A. Noninvasive imaging of apoptosis and its application in cancer therapeutics. Clin Cancer Res. 2008; 14:2492–2501. [PubMed: 18413842]
36. Elkabets M, Vora S, Juric D, Morse N, Mino-Kenudson M, Muranen T, et al. mTORC1 inhibition is required for sensitivity to PI3K p110alpha inhibitors in PIK3CA-mutant breast cancer. Science translational medicine. 2013; 5:196ra99.
37. Montano R, Thompson R, Chung I, Hou H, Khan N, Eastman A. Sensitization of human cancer cells to gemcitabine by the Chk1 inhibitor MK-8776: cell cycle perturbation and impact of administration schedule in vitro and in vivo. BMC Cancer. 2013; 13:604. [PubMed: 24359526]
38. Bean JR, Hosford SR, Symonds LK, Owens P, Dillon LM, Yang W, et al. The PI3K/mTOR dual inhibitor P7170 demonstrates potent activity against endocrine-sensitive and endocrine-resistant ER+ breast cancer. Breast Cancer Res Treat. 2014
39. Chakrabarty A, Sanchez V, Kuba MG, Rinehart C, Arteaga CL. Feedback upregulation of HER3 (ErbB3) expression and activity attenuates antitumor effect of PI3K inhibitors. Proc Natl Acad Sci U S A. 2012; 109:2718–2723. [PubMed: 21368164]
40. Hata AN, Yeo A, Faber AC, Lifshits E, Chen Z, Cheng KA, et al. Failure to induce apoptosis via BCL-2 family proteins underlies lack of efficacy of combined MEK and PI3K inhibitors for KRAS-mutant lung cancers. Cancer Res. 2014; 74:3146–3156. [PubMed: 24675361]

41. Certo M, Del Gaizo Moore V, Nishino M, Wei G, Korsmeyer S, Armstrong SA, et al. Mitochondria primed by death signals determine cellular addiction to antiapoptotic BCL-2 family members. Cancer Cell. 2006; 9:351–365. [PubMed: 16697956]

Statement of Translational Relevance

One-third of patients with estrogen receptor α (ER)-positive breast cancer develop anti-estrogen-resistant disease that is virtually incurable. Activation of the phosphatidylinositol 3-kinase (PI3K) pathway promotes anti-estrogen resistance. Combinations of anti-estrogens and PI3K inhibitors are being developed, however, mechanistic understanding of the temporal effects is lacking, which is critical to inform rational treatment scheduling. Given that PI3K inhibitor treatment regimens being tested clinically provide continuous drug exposure, induce significant toxicity, and inconsistently provide robust pathway inhibition, we sought to determine whether anti-tumor efficacy could be achieved using pharmacodynamically-informed treatment schedules. Different treatment schedules of a PI3K inhibitor elicited different patterns of pathway inhibition/reactivation, apoptosis, and proliferative inhibition/hyperactivation, while all eliciting therapeutic tumor responses. Clinical testing of different PI3K inhibitor treatment schedules is warranted to reduce toxicity while preserving efficacy. Furthermore, the concept of transient pathway interruption to increase therapeutic index may be extrapolated to the development of other signaling pathway modulators.

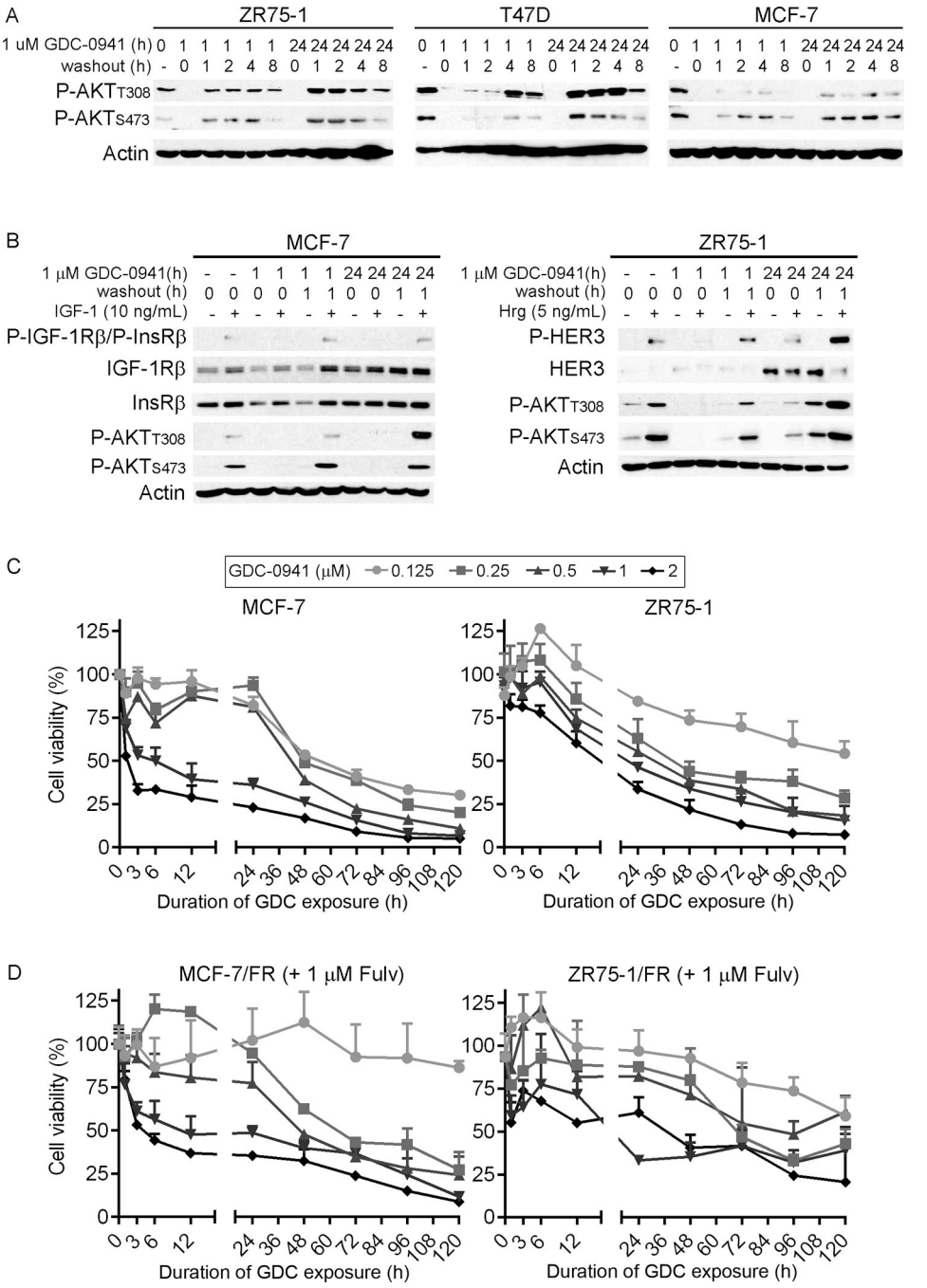

Figure 1. Transient, complete inhibition of PI3K more effectively suppresses cell growth than chronic, partial inhibition

A) Cells were treated with GDC-0941 for 0, 1, or 24 h, then drug was washed out. Lysates were collected 0, 1, 2, 4, or 8 h post-washout, and analyzed by immunoblotting using the indicated antibodies. B) Cells were serum-starved for 16–24 h, and co-treated with GDC-0941 for 0, 1, or 24 h. After 0 or 1 h of drug washout, cells were stimulated +/− IGF-1 or heregulin (Hrg) for 5 min, then lysed. Lysates were analyzed as in (A). C–D) Cells were treated with 0–1 μM GDC-0941 at time point "0," and drug was washed out after 0–120 h.

In (D), cells were treated with 1 μM fulv. Relative viable cell numbers were measured at 120 h. Data are shown as mean of triplicates + SD.

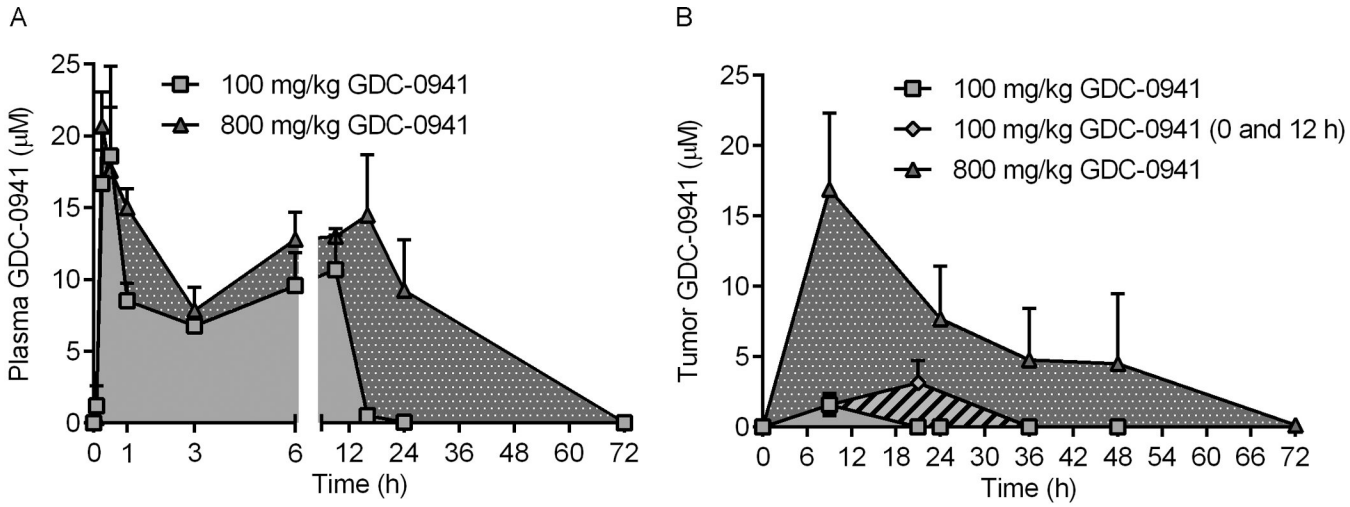

Figure 2. Pharmacokinetic analysis of GDC-0941

A) Mice were treated with GDC-0941. Blood was collected at the indicated time points after drug administration, and plasma was used to measure GDC-0941 levels. B) Mice bearing MCF-7 tumors were pretreated with fulv, then treated 3 d later with GDC-0941. Tumors harvested at the indicated time points were used to measure GDC-0941 levels. An additional group of mice was treated with a second dose of GDC-0941 (100 mg/kg) at 12 h. Data are presented as mean of triplicates + SD.

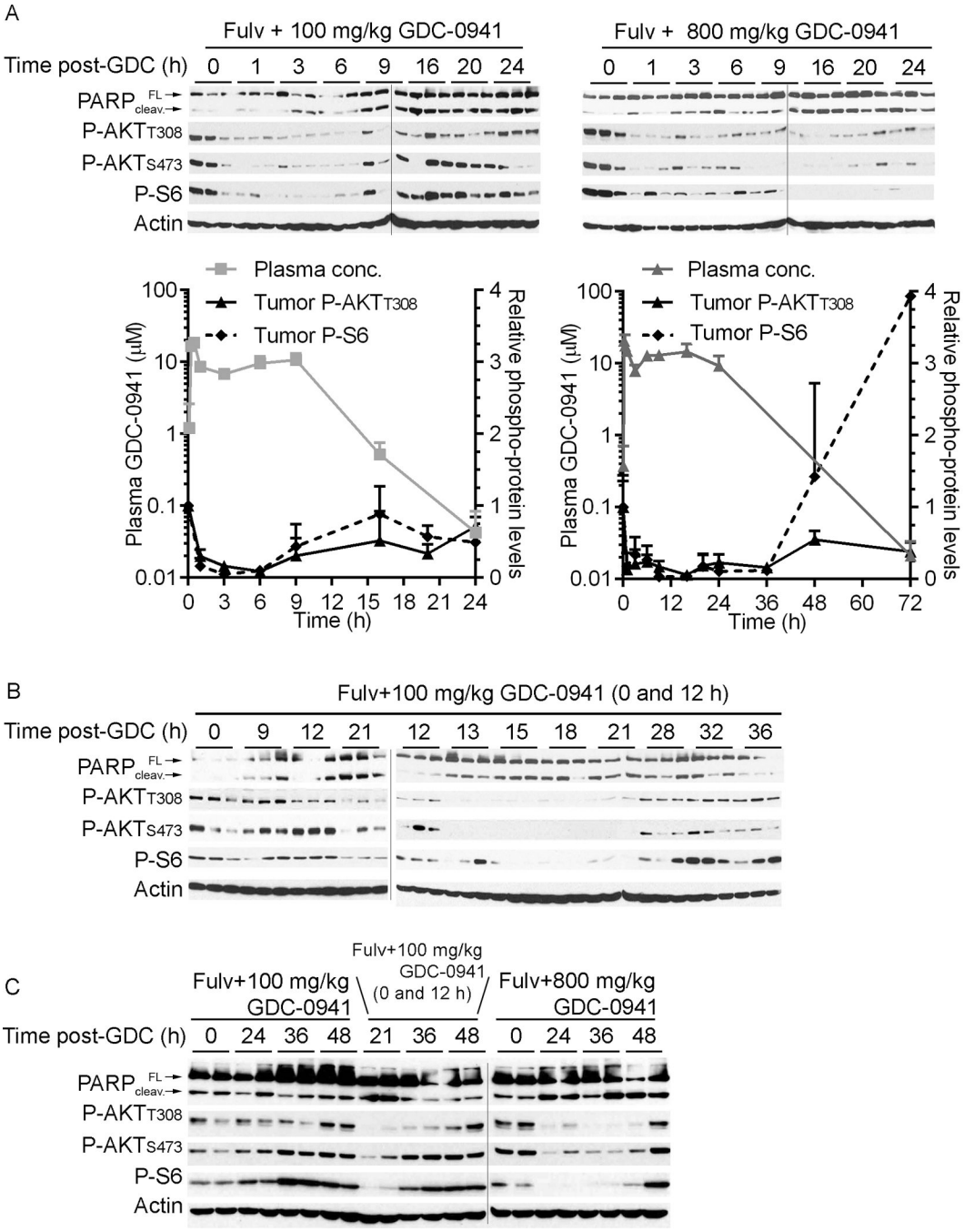

Figure 3. Pharmacodynamic effects of GDC-0941 with fulv on MCF-7 tumors

Mice were pretreated with fulv. Three days later, mice were treated with (A,C) one or (B,C) two doses of GDC-0941 as indicated. Tumors were harvested at 0–48 h after GDC-0941 treatment, and lysates were analyzed by immunoblotting using the indicated antibodies. In (A), phosphoprotein levels quantified by densitometry of immunoblots (normalized to 0 h time point) were plotted against plasma GDC-0941 levels from Fig. 2A. Data are shown as mean of triplicate tumors + SD. FL- full-length; cleav.- cleaved.

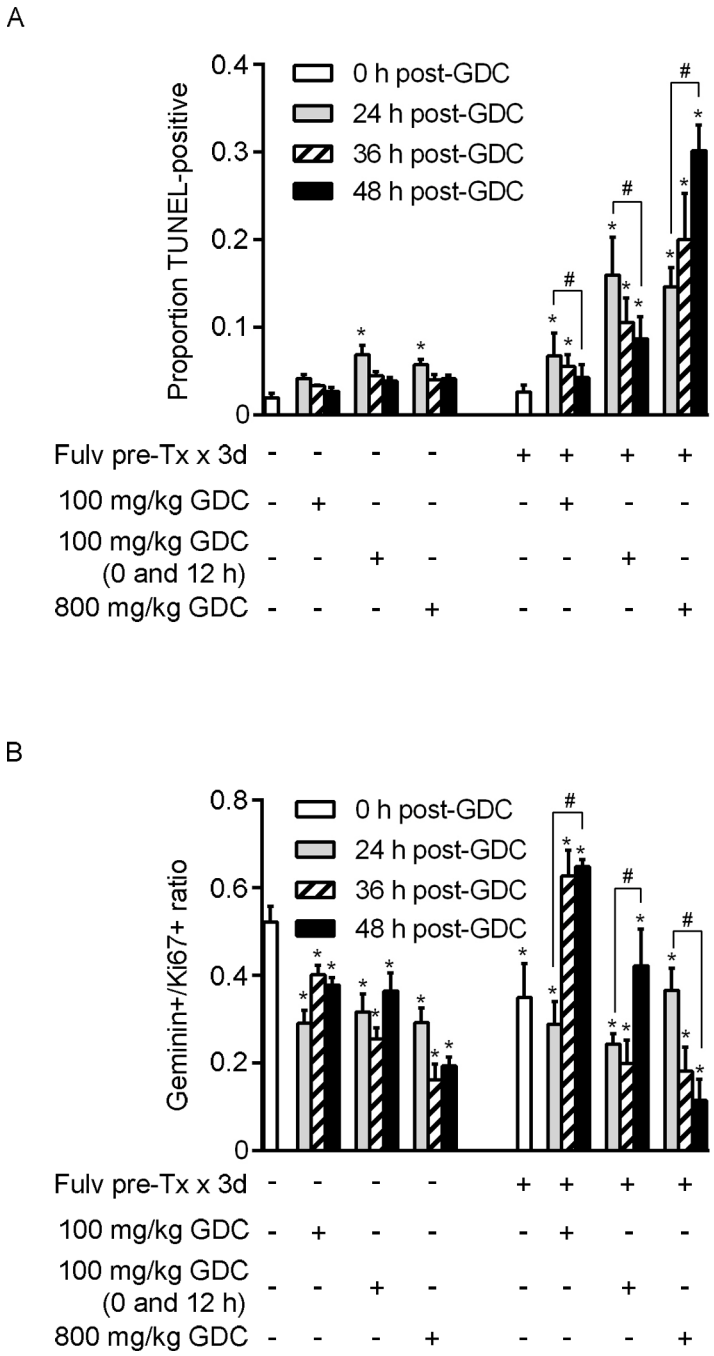

Figure 4. Intermittent, longer-term PI3K inhibition increases tumor cell apoptosis and suppresses proliferation in combination with anti-estrogen therapy

Mice were pretreated with fulv 3 d before treatment with one or two doses of GDC-0941 as indicated. Tumors were harvested at 0–48 h after GDC-0941 treatment, and analyzed by (A) TUNEL to assess apoptosis, or (B) IHC for geminin and Ki67 to assess cell proliferation. Geminin:Ki67 ratios were calculated. Data are shown as mean of triplicate tumors + SD. *$p \leq 0.05$ compared to baseline controls. #$p \leq 0.05$ by Bonferonni post-hoc test as indicated with brackets.

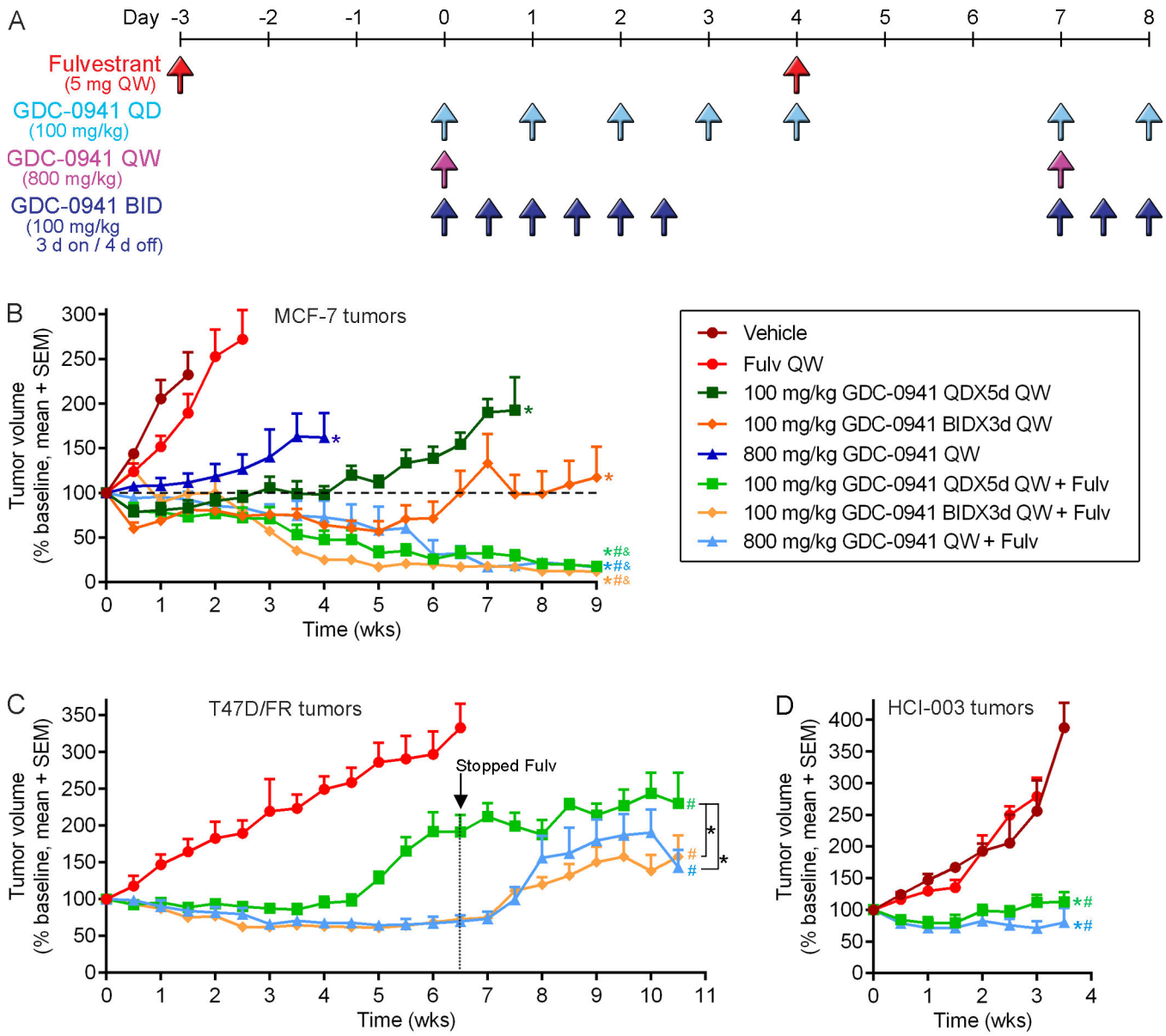

Figure 5. Intermittent, longer-term PI3K inhibition is as effective as metronomic inhibition in combination with anti-estrogen therapy for ER+ breast cancer

Mice (n=7–9/group) bearing (B) MCF-7 tumors, (C) T47D/FR tumors, or (D) HCI-003 patient-derived xenografts were treated as indicated in (A). In (C), mice were treated with fulv starting at the time of xenografting, and fulv was stopped after 6.5 wk of GDC-0941/fulv treatment. Mean + SEM is shown. *$p \leq 0.05$ compared to vehicle-treated group, or as indicated with brackets. $^{\#}p \leq 0.05$ compared to fulvestrant-treated group. $^{\&}p \leq 0.05$ compared to GDC-0941-treated group at same dose/schedule. Statistical analysis of (B) included data up to 6.5 wk.

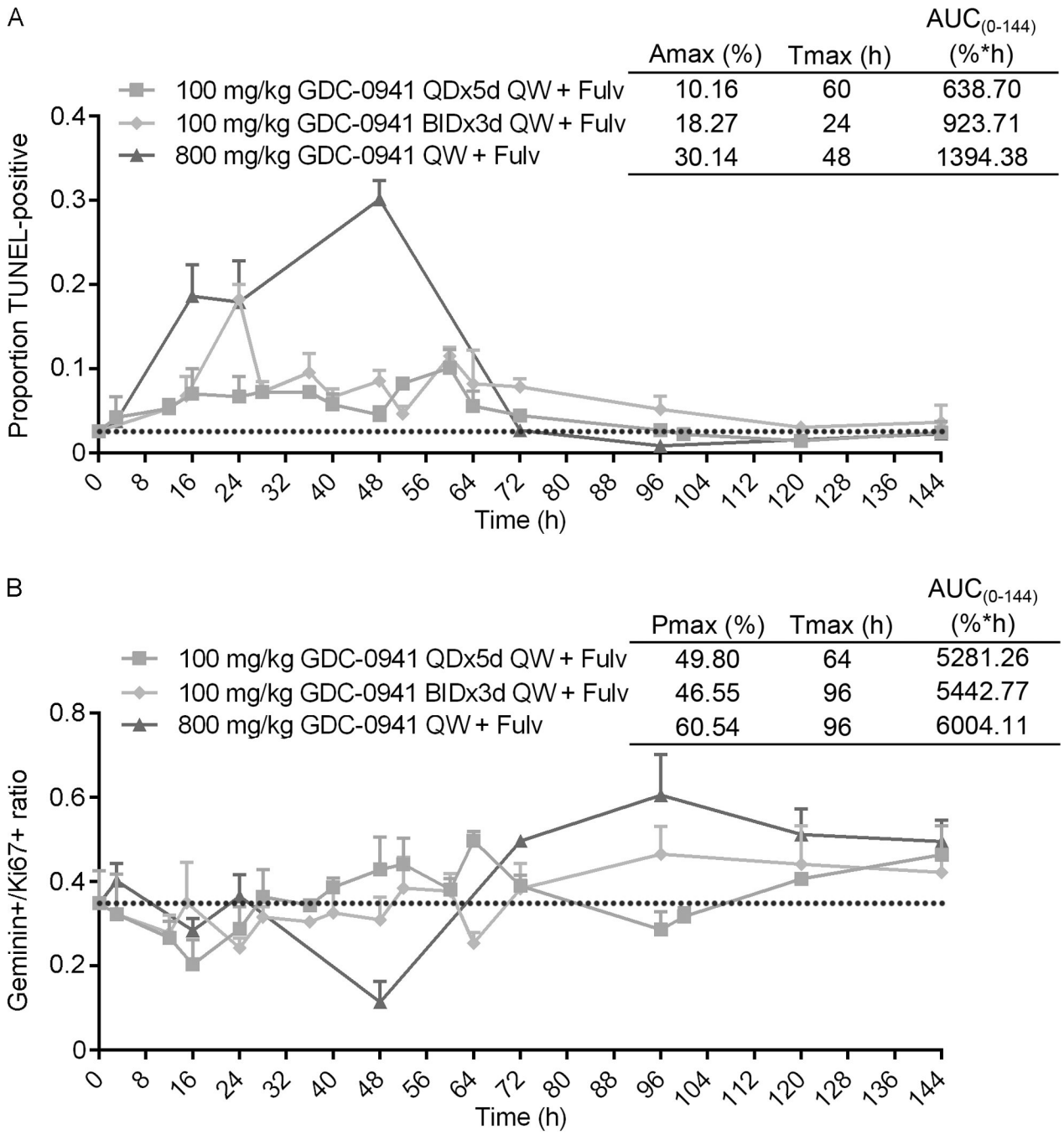

Figure 6. Intermittent, longer-term inhibition of PI3K and ER induces a bolus of tumor cell apoptosis and suppression of proliferation, with proliferative rebound after recovery of PI3K activity

Mice were treated as in Fig. 5, and tumors were analyzed by IHC and TUNEL as in Fig. 4. Data are shown as mean of triplicate tumors + SD. Pharmacodynamic modeling was used to calculate maximum impact (Amax for apoptosis; Pmax for proliferation), time to maximum impact (Tmax), and area under the curve from 0–144 h [$AUC_{(0–144)}$].